



Published in final edited form as:

J Biol Inorg Chem. 2013 February ; 18(2): 223–232. doi:10.1007/s00775-012-0967-z.

Coordination of peroxide to the Cu_M center of peptidylglycine α-hydroxylating monooxygenase (PHM): structural and computational study

Katarzyna Rudzka,

Department of Biophysics and Biophysical Chemistry, Johns Hopkins School of Medicine, Johns Hopkins University, Baltimore, MD 21205, USA

Diego M. Moreno,

Department of Inorganic, Analytical and Physical Chemistry, University of Buenos Aires, Buenos Aires, Argentina

Betty Eipper,

Department of Neuroscience and Molecular, Microbial and Structural Biology, University of Connecticut Health Center, Farmington, CT 06030, USA

Richard Mains,

Department of Neuroscience and Molecular, Microbial and Structural Biology, University of Connecticut Health Center, Farmington, CT 06030, USA

Dario A. Estrin, and

Department of Inorganic, Analytical and Physical Chemistry, University of Buenos Aires, Buenos Aires, Argentina

L. Mario Amzel

Department of Biophysics and Biophysical Chemistry, Johns Hopkins School of Medicine, Johns Hopkins University, Baltimore, MD 21205, USA

L. Mario Amzel: mamzel@jhmi.edu

Abstract

Many bioactive peptides, such as hormones and neuropeptides, require amidation at the C terminus for their full biological activity. Peptidylglycine α-hydroxylating monooxygenase (PHM) performs the first step of the amidation reaction—the hydroxylation of peptidylglycine substrates at the C_α position of the terminal glycine. The hydroxylation reaction is copper- and O₂-dependent and requires 2 equiv of exogenous reductant. The proposed mechanism suggests that O₂ is reduced by two electrons, each provided by one of two nonequivalent copper sites in PHM (Cu_H and Cu_M). The characteristics of the reduced oxygen species in the PHM reaction and the identity of the reactive intermediate remain uncertain. To further investigate the nature of the key

© SBIC 2012

Correspondence to: L. Mario Amzel, mamzel@jhmi.edu.

An interactive 3D complement page in Proteopedia is available at <http://proteopedia.org/w/Journal:JBIC:18>

Electronic supplementary material The online version of this article (doi:10.1007/s00775-012-0967-z) contains supplementary material, which is available to authorized users.

intermediates in the PHM cycle, we determined the structure of the oxidized form of PHM complexed with hydrogen peroxide. In this 1.98-Å-resolution structure (hydro)peroxide binds solely to Cu_M in a slightly asymmetric side-on mode. The O–O interatomic distance of the copper-bound ligand is 1.5 Å, characteristic of peroxide/hydroperoxide species, and the Cu–O distances are 2.0 and 2.1 Å. Density functional theory calculations using the first coordination sphere of the Cu_M active site as a model system show that the computed energies of the side-on L₃Cu_M(II)–O₂²⁻ species and its isomeric, end-on structure L₃Cu_M(I)–O₂^{·-} are similar, suggesting that both these intermediates are significantly populated within the protein environment. This observation has important mechanistic implications. The geometry of the observed side-on coordinated peroxide ligand in L₃Cu_M(II)O₂²⁻ is in good agreement with the results of a hybrid quantum mechanical–molecular mechanical optimization of this species.

Keywords

Peptidylglycine α-hydroxylating monooxygenase; Peroxide; Amidation of peptides; Copper-containing proteins

Introduction

Peptidylglycine α-hydroxylating monooxygenase (PHM) plays a key role in the conversion of glycine-extended peptide precursors into mature neuropeptides and growth factors amidated at their C terminus. It performs hydroxylation at the Cα position of the terminal glycine of peptidylglycine substrates, the first step in the two-step amidation reaction [1–3]. The subsequent N-dealkylation, catalyzed by peptidyl-α-hydroxyglycine α-amidating lyase (PAL), yields the α-amidated peptides (Scheme 1). In vertebrates PHM and PAL are expressed as one bifunctional protein, peptidylglycine α-amidating monooxygenase (PAM), but the two enzymes retain their enzymatic activities when expressed individually or separated by endoproteolytic cleavage [4–8]. Amidation of the C terminus is frequently required for the full biological activity of neuropeptides, and PAM is the only enzyme known to catalyze this reaction [9–11].

The structure and the mechanism of the catalytic core of PHM (PHMcc; rat PAM-1, residues 42–356) have been studied in detail by multiple techniques, including X-ray diffraction [12–15], Fourier transform infrared spectroscopy [16–18], circular dichroism/magnetic circular dichroism [19], electron paramagnetic resonance [19–21], X-ray absorption spectroscopy [17, 18, 20, 22], and the kinetic isotope effect [23–26].

X-ray diffraction studies showed that PHM is composed of two domains separated by a large solvent-filled cavity [12]. Two copper ions (Cu_H and Cu_M), one bound to each PHM domain, are necessary for the enzymatic activity. PHM is often referred to as a noncoupled dinuclear copper enzyme, since the spatial separation of the domains results in no direct interaction between the metal sites [19]. Crystallographic, biochemical, and spectroscopic evidence points to different roles for each copper site in the reaction cycle: whereas Cu_M serves as an oxygen-activation and hydrogen-abstraction site, Cu_H provides the second electron for the two-electron reduction.

In the resting state, both active sites of PHM contain Cu(II) (oxidized form of PHM, oxPHM). Reaction with 2 equiv of ascorbate generates the catalytically competent reduced Cu(I)-containing PHM. The reduced Cu_M site is then capable of binding molecular oxygen; however, binding of O₂ requires the presence of the peptide substrate [13, 25, 27]. The X-ray structure of the ternary complex of reduced PHMcc with dioxygen and the slow-reacting peptide substrate *N*-acetyldiiodotyrosyl-*b*-threonine showed the arrangement of substrates prior to catalysis (Fig. 1) [13]. In this precatalytic complex, dioxygen is coordinated end-on to Cu_M with a Cu–O–O angle of 110° and an O–O interatomic distance of 1.23 Å. The position of the distal oxygen with respect to the C α atom of the peptide suggests the involvement of the copper-bound oxygen species in the hydrogen-abstraction process. Formation of this ternary complex is followed by the electron transfer from Cu_H to the copper-bound oxygen. Given the long distance that separates the metal sites (11 Å; Fig. 2), identifying the pathway for electron transfer from Cu_H to Cu_M–O₂ has been challenging. Several hypotheses for the long-range electron transfer in PHM have been formulated [13, 23, 28, 29]. On the basis of crystallographic studies, Prigge et al. [13] suggested that the peptide substrate bound close to Cu_M provides a path for the electron transfer. Other experimental evidence was interpreted as suggesting different electron transfer paths, but thus far the kinetic and spectroscopic studies provide conflicting results.

Another unresolved aspect of the mechanism is the identity of the reactive intermediate that abstracts the glycine C α hydrogen atom from the peptidylglycine substrate. The reactivity of one- and two-electron-reduced Cu/O₂ intermediates towards hydrogen-atom abstraction has been evaluated in several studies [29–32]. Applying density functional theory (DFT) methods in PHM small-model systems, Chen and Solomon [33] calculated the activation barriers for the hydrogen-abstraction step considering two possible reactive species: Cu_M(II)–superoxo—L₃Cu_M(II)–O^{•−}—and Cu(II)–hydroperoxo—L₃Cu_M(II)–OOH[−]. The results suggested that the Cu_M(II)–superoxo intermediate should be more effective in hydrogen-atom abstraction than Cu_M(II)–hydroperoxide (reaction barrier 14 vs. 37 kcal/mol, respectively). These calculations were revisited by Crespo et al. [28], who used a whole-enzyme model in the quantum mechanical (QM)–molecular mechanical (MM) calculations. They found that the activation barriers for the hydrogen abstraction by Cu_M(II)–superoxo were considerably higher than those calculated by Chen and Solomon (20 kcal/mol for the singlet and 25 kcal/mol for the triplet) and argued that this species is not likely to act as a reactive intermediate. Similarly to Chen and Solomon's studies, Crespo et al. ruled out the participation of Cu_M(II)–hydroperoxide in the hydrogen-abstraction process. Additionally, they proposed that the spontaneous protonation of L₃Cu_M(II)–OOH[−] and the subsequent release of water results in the formation of a monooxygenated intermediate that might promote the hydrogen abstraction. This is also consistent with calculations performed for the related dopamine β -monooxygenase protein [34].

Although there is no consensus on the role of copper-bound hydroperoxide in the reaction cycle of PHM, it is generally accepted that L₃Cu_M(II)–OO(H)[−] may be one of the key intermediates in the reaction mechanism. In this work we report the formation and the structural characterization of the oxPHM complexed with hydrogen peroxide. Treatment of crystalline oxidized PHMcc (oxPHMcc) with a solution of hydrogen peroxide results in

capture of a Cu_M -coordinated (hydro)peroxide species with side-on coordination. In addition, we performed DFT calculations using the first coordination sphere of the Cu_M active site as a partial model system. Taking into account different protonation states, we computed the geometrical parameters of Cu_M -bound peroxide species. An optimized model of Cu_M and its three side chain ligands, containing a doubly deprotonated peroxy species, correlates best with our X-ray diffraction results.

Comparison of the relative energies associated with the side-on species, which can be described as $\text{L}_3\text{Cu}_M(\text{II})-\text{O}_2^{2-}$, with those of its isomeric end-on structure $\text{L}_3\text{Cu}_M(\text{I})-\text{O}_2^-$ suggests that these two isomeric moieties are significantly populated at equilibrium within PHM protein. In addition to the mechanistic relevance of PHM-(hydro)peroxide, this complex is also important from a strictly structural point of view, since X-ray structures of peroxide species in non-heme copper proteins are scarce [35–37].

Materials and methods

Protein production and crystallization

Stably transfected Chinese hamster ovary cells secreting PHM (PHMcc, residues 42–356) were constructed using the pCIS vector system [38]. PHM protein was harvested from the culture medium by precipitation with $(\text{NH}_4)_2\text{SO}_4$ and purified as described previously [12]. The protein solution was concentrated to 12 mg/ml, mixed with an equal volume of mother liquor (0.38 mM CuSO_4 , 1.2 mM NiSO_4 , 3 mM NaN_3 , 100 mM sodium cacodylate pH 5.5), and crystallized by hanging-drop diffusion.

Preparation of oxPHMcc- H_2O_2 crystals

Single crystals of oxPHMcc were transferred from the mother liquor to a drop containing 1.6 mM NiSO_4 , 100 mM sodium cacodylate pH 5.5 to remove the excess copper ions. The PHM- H_2O_2 complex was obtained by soaking the crystals in a solution of the mother liquor with 10 mM H_2O_2 and 20 % glycerol for 3 min. For data collection, the H_2O_2 -soaked crystals were flash frozen in a stream of nitrogen gas (100 K).

Data collection, structure determination, and refinement

X-ray diffraction data were collected at beamline X6A of the National Synchrotron Light Source. Frames were processed with the HKL2000 software package [39]. Data were indexed and integrated in space group $P2_12_12_1$ on the basis of the diffraction symmetry, the systematic absences, and the equivalence with previous PHM crystals [12, 13]. The structure was determined by molecular replacement with the program MOLREP using the coordinates of the native enzyme (Protein Data Bank, PDB, file 1SDW.pdb) as the search model. The model was built and refined using REF-MAC 5.0 as implemented in the CCP4 suite of programs [40, 41]. During the refinement process, the O–O interatomic distance of the ligand coordinated to Cu_M was initially set to 1.469 Å, corresponding to the distance characteristic of a peroxide molecule. However, to avoid model bias in the refinement, a low weight was given to the distance constant (weight = $1/\sigma^2$, with $\sigma = 0.08$ Å). Refinement was monitored by calculating the R value and the R_{free} value calculated using 5 % of the reflections set aside for cross-validation.

DFT calculations

Model system calculations were performed within the DFT framework using the Perdew–Burke–Ernzerhof exchange–correlation functional of the Gaussian 03 package [42], using the 6–31G* basis set. In addition to the 6–31G* basis set, the O–O interatomic distance of the peroxide ligand was calculated using the TZVP basis set (Table S2).

Mulliken and atoms in molecules (AIM) [43] populations were computed to describe the charge distribution of the species investigated. Hybrid QM–MM calculations were performed using an implementation [44] in which the QM subsystem is treated at the density functional level using the program SIESTA [45]. For all atoms, basis sets of double- ζ plus polarization quality were employed, with a pseudoatomic orbital energy shift of 30 meV and a grid cutoff of 150 Ry [45, 46]. Calculations were performed using the generalized gradient approximation functional proposed by Perdew et al. [47]. This combination of functional, basis sets, and grid parameters was validated in our previous work [28]. The classical subsystem was treated using the Amber99 force field parameterization [48]. The initial structure was taken from the experimental X-ray data. Copper plus the coordinated side chains of residues His242, His244, and Met314 and the two oxygen atoms in the ligand were selected as the quantum subsystem, which comprises 30 atoms. The rest of the protein was treated classically. We allowed free motion for QM atoms located inside a sphere of 13.5 Å from the center of mass of the QM subsystem. The frontier between the QM and MM portions of the system was treated by the SPLAM link atom method [49].

Results and discussion

ox-PHMcc–peroxide complex

Crystals of oxPHMcc were soaked for 3 min in mother liquor containing 10 mM H₂O₂ before they were frozen in a stream of 100 K N₂ gas. X-ray diffraction data were collected to 1.98-Å resolution (Table 1). Electron density maps confirmed that the (hydro)peroxide anion coordinates Cu_M of PHM, displacing the water ligand found in the resting state of the enzyme. (Hydro)peroxide binds to copper in a slightly asymmetric side-on mode. The Cu–O distances refined to 2.0 and 2.1 Å and the O–O bond refined to 1.5 Å (Figs. 3, 4). The temperature factors of the oxygen atoms (45.4 and 47.2) were comparable to the average value of the temperature factors of all atoms in the structure (46.1), indicating that the peroxide ligand is present in the crystal with full occupancy. (Extensive tests of the possibility of the presence of a partially occupied end-on ligation suggested by the QM calculations indicated that this form, if present, would have less than 0.3 occupancy.) The O–O interatomic distance is characteristic of a peroxide/hydroperoxide species and is significantly longer than the distance typically observed in superoxide [13, 50]. The η^2 -Cu–O₂ arrangement forms two acute angles: 64.1° and 71.9°. The Cu_M-bound side-on peroxide molecule is stabilized by hydrogen-bonding interactions with a water molecule (distances of 3.0 and 2.6 Å).

The structure of the peroxide-soaked PHM does not differ noticeably from that of the native protein except for a large change in the conformation of the Cys126–Thr130 loop: the loop shifts approximately 8 Å towards the Cu_M site with respect to its position in the absence of

H₂O₂. The amino acid residues of the shifted region are present in the structure with nearly full occupancy. We also obtained a lower-resolution X-ray diffraction data set (2.15 Å) from a crystal prepared under the same experimental conditions (data not shown). This data set shows that the peroxide ligand binds to the Cu_M site in the same fashion as we observed in the 1.98-Å structure. However, in the lower-resolution data set, the predominant conformation adopted by the Cys126–Thr130 loop is identical to that of the peroxide-free protein. These results indicate that the conformational variation within the Cys126–Thr130 loop does not correlate with the coordination of the peroxide ligand.

In the oxPHMcc–peroxide complex the Cu_M ligands—His242, His 244, Met314, and the (hydro)peroxide molecule—form a distorted tetrahedron, as was observed in the previously determined structures of PHMcc [12–14] (with a water molecule instead of peroxide at the fourth position). Cu_H is coordinated by three histidine residues (His 107, His108, and His 172) and has planar, distorted T-shape geometry with one unoccupied coordination position (Fig. 2). Our data indicate that (hydro)peroxide does not perturb the ligation of the Cu_H site and coordinates exclusively to the Cu_M site. These results agree with our recent studies that showed that small molecules such as nitrite, azide, and carbon monoxide do not bind to Cu_H in PHM, although they have been shown to bind to copper sites in other systems [51]. This led us to suggest that the coordination of small molecules at the Cu_H site is prevented by the protein since ligands might disrupt the fine-tuning of the redox potential of Cu_H required to perform its role in electron transfer [51].

Model system and QM–MM calculations

QM optimization of the Cu_M site with coordinated peroxide was performed using the coordinates of the PHM-H₂O₂ crystal structure as a starting point. The copper ion of the Cu_M site, the side chains of the first coordination sphere (His242, His244, and Met314), and (hydro)peroxide were included in the DFT calculations. Different protonation states of the peroxide ligand were considered. In the optimized model of Cu_M complexed with H₂O₂—L₃Cu_M(II)–H₂O₂—the distance from the metal center to the distal oxygen of peroxide was 2.68 Å (Table 2); a similar distance was obtained when the structure contained monoprotonated peroxide ligand—L₃Cu_M(II)–HO₂[−], Cu–O(distal) distance 2.82 Å—significantly longer than the experimental distances. In contrast, when the doubly deprotonated ligand (O₂^{2−}) was used, both calculated Cu_M–O distances were 1.95 Å, highly similar to those observed in the experimental structure. When the 6–31G* basis set was used to optimize the O–O bond of the O₂^{2−} ligand, the calculated distance was 1.44 Å, which agreed well with the experimental distance of 1.5 Å. A change in the basis set from 6–31G* to TZVP did not have a significant influence on the O–O bond distance (Table S2). Furthermore, Cu(II)-bound peroxo species interacts closely with a molecule of water, forming two hydrogen bonds. To examine the effect of hydrogen bonding on the O–O distance in the peroxide ligand, we optimized the Cu_M site including a hydrogen-bonded water molecule. The geometrical parameters of the L₃Cu_M(II)–O₂^{2−}–H₂O system are nearly identical to those of the previously optimized system, indicating that the hydrogen bonding has no significant effect on the calculated O–O bond distance (Fig. S1, Table S1). When the relative energies of the side-on species L₃Cu_M(II)–O₂^{2−} and its isomeric end-on structure L₃Cu_M(I)–O₂[−] were calculated, the two systems appeared to be nearly isoenergetic, with

the side-on species 1.1 kcal/mol higher in energy than the end-on complex. These results strongly suggest that end-on and side-on species could coexist in the PHM protein. Analysis of the Mulliken and AIM populations indicates, as expected, that the side-on species has a significant contribution of $L_3Cu_M(II)O_2^{2-}$ structure. The Mulliken charges for the copper atom and the two oxygen atoms in the side-on structure were $0.57e$, $-0.40e$, and $-0.36e$, whereas the AIM charges were $0.95e$, $-0.59e$, and $-0.52e$. The end-on structure has a larger contribution of $L_3Cu_M(I)O^-$ structure, with Mulliken populations of $0.45e$, $-0.34e$, and $-0.29e$ and AIM populations of $0.80e$, $-0.52e$, and $-0.32e$.

QM-MM optimizations of both side-on and end-on structures of the copper-bound doubly deprotonated peroxide moiety show that the side-on coordinated structure agrees very well with the experimental results, confirming that O_2^{2-} is the coordinated species in the oxPHMcc-H₂O₂ structure (Table 2, Fig. 5).

Mechanism of the PHM-catalyzed reaction

Despite spectroscopic and structural evidence provided by small model systems, the role of (hydro)peroxide-bound PHM in the catalytic mechanism is still not clear. As Bauman et al. [52] pointed out, if $L_3Cu_M(II)$ -(hydro)peroxide is capable of catalyzing the hydroxylation of a peptidylglycine substrate, the oxPHM should be able to use H₂O₂ to generate the hydroxylated product. Isotope labeling experiments suggested that oxPHM is indeed capable of performing the hydroxylation of substrates using H₂O₂ as the only source of oxygen and reducing equivalents. In an experiment in which ¹⁸O-labeled peroxide was reacted with substrate in the presence of PHM under anaerobic conditions, Bauman et al. [52] observed the nearly quantitative incorporation of the labeled oxygen into the product. This reactivity resembles the “peroxide shunt” that has been previously observed in other oxygenases, such as cytochrome P-450, methane monooxygenase, and naphthalene 1,2-dioxygenase [53–56]. It has been demonstrated that these enzymes are capable of using hydrogen peroxide to generate the hydroxylated products via an O₂-independent pathway. In the PHM-catalyzed reaction, full incorporation of label was also observed when both peroxide and oxygen labeled with ¹⁸O were used. However, when peroxide labeled with ¹⁸O was reacted with PHM and substrate in the presence of ¹⁶O₂, only 35 % of the product showed ¹⁸O incorporation. This significant scrambling of labeled oxygen indicates that an intermediate exists that allows exchange of ¹⁸O with atmospheric oxygen. Bauman et al. suggested that the reactivity of PHM triggered by H₂O₂ and the O₂-dependent route intersect in a common intermediate, most likely copper superoxide. They further proposed that copper superoxide, not copper (hydro)peroxide, might act as a reactive species in the hydrogen-abstraction reaction.

The structure of Cu(II)-PHM in complex with H₂O₂ presented here shows a stable species consisting of a side-on Cu-O₂ center with short Cu-O distances (2.0 and 2.1 Å) and a long O-O distance (1.49–1.50 Å). These features, and the method of preparation, suggest that this structure corresponds to a Cu(II)-PHM-bound reduced oxygen species—peroxidoate—or singly or doubly protonated hydroperoxide.

The QM and QM-MM calculations are only compatible with a doubly deprotonated species (O_2^{2-}). The calculations also indicate that side-on copper(II) peroxide and its isomeric form,

the end-on copper(I) superoxide complex, have similar energies and therefore they may interconvert during the catalytic cycle. The mechanism supported by these observations and previously published data suggests that in the presence of substrate O_2 binds to $L_3Cu_M(I)$ in an end-on fashion. This species is in resonance with $L_3Cu_M(II)O_2^{\cdot-}$. Transfer of an electron from $Cu_H(I)$ yields an end-on $L_3Cu_M(I)-O_2^{\cdot-}$ that can convert into its isoenergetic form, the side-on $L_3Cu_M(II)-O_2^{2-}$. Protonation of this form causes the release of a water molecule, leaving a highly reactive $Cu_M(III)$ -oxyl species that abstracts $H\cdot$ from the $C\alpha$ of the glycine residue [57] (Scheme 2). The resulting glycine radical reacts with the $L_3Cu_M(III)$ -hydroxyl complex to generate a $Cu_M(II)$ -bound alcoholate. Addition of a water molecule releases the alcoholate in the form of the hydroxylated product and regenerates the $Cu_M(II)-OH(H)$ form of the enzyme. This mechanism is compatible with the kinetic isotope effect data of Miller and Klinman [58] that in the case of dopamine β -monooxygenase (a mechanistic analog of PHM [25]) were interpreted as suggesting that homolytic breakage of the $O-O$ bond occurs before breakage of the $C-H$ bond. However, more recent data from the Klinman group [23, 26] showed the dependence of the ^{18}O kinetic isotope effect on deuteration of the substrate, which argues that the $C-H$ bond cleavage precedes the cleavage of the $O-O$ bond. This led the Klinman group to propose that $Cu(II)-O_2^{\cdot-}$ is the species that abstracts the hydrogen from the substrate, forming the $Cu(II)-OOH$ intermediate. If this mechanism is operational, hydroxylation using H_2O_2 would have to occur by a different mechanism because the $Cu(II)-OOH$ species is formed after hydrogen abstraction.

Although not all steps of the PHM-catalyzed mechanism are well understood and some aspects are still a subject of much debate, it is commonly accepted that a copper-bound (hydro)peroxide species is generated in the PHM reaction. The structure of the oxPHM-peroxide complex presented herein can offer a basis for future experimental and computational efforts.

Structural mimics of the oxPHMcc-peroxide structure

The oxPHMcc-peroxide complex described in this work is a unique example of a coordination mode of a (hydro)peroxide ligand to the copper site of a protein. In contrast to the structures reported thus far, in H_2O_2 -soaked PHM, the O_2^{2-} ligand exhibits a side-on mode of binding with two nearly identical $Cu-O$ distances. Although no precedent exists for such a binding mode among non-heme copper proteins, the possibility of rearrangement of an end-on hydroperoxo ligand to a side-on coordination has been examined in small molecule model chemistry. The findings of low-temperature stopped-flow studies of the reaction of copper(II) complexes with H_2O_2 [59] were interpreted as indicating that the initially formed end-on hydroperoxo ligand rearranges into a side-on peroxo ligand to give a copper(II)-peroxo complex. In bioinorganic chemistry there has been much interest in understanding how O_2/H_2O_2 -derived species interact with copper sites. Dinuclear complexes containing a bridging peroxo moiety were the first to be well described [60]. Preparation and characterization of mononuclear copper-(hydro)peroxo adducts is a synthetic challenge, since the primary products tend to dimerize, forming dinuclear peroxo-bridged complexes. Nevertheless, a number of well-characterized complexes supported by sterically hindered ligand systems have been synthesized and studied extensively [61–64].

Structures of proteins containing copper–oxygen centers

The short-lived intermediates formed in the reaction of copper enzymes with reduced oxygen species have been difficult to characterize using crystallographic methods. To date only a few X-ray structures of such complexes have been reported. The X-ray structure of superoxide dismutase from *Alvinella pompejana* in the presence of the reaction product (H_2O_2) has been determined (PDB accession code 3F7K) [37]. In this structure, determined to 1.35-Å resolution, hydroperoxide binds weakly to the copper center (Cu–O distance of 2.75 Å) in an end-on fashion. Analysis of this structure allowed the Shin et al. [37] to suggest a unified inner-sphere mechanism for superoxide dismutase catalysis that involves movement of the metal. A similar weak interaction of a copper site with a reduced oxygen species, believed to be a (hydro)peroxide reaction product, was observed by Wilmot et al. [65, 66] in the structure of amine oxidase (PDB accession code 1D6Z). X-ray diffraction experiments performed under catalytic conditions allowed amine oxidase to be trapped in a complex with a peroxide species. In that structure the O_2 -derived species binds in the active site [Cu(II)–O bond distance of 2.8 Å] and interacts through hydrogen bonding with the iminoquinone cofactor. Formation of these hydrogen bonds points to the anionic character of the oxygen-derived ligand in amine oxidase; however, the O–O interatomic distance refined to 1.26 Å, much shorter than the typical peroxide bond.

In addition to the structures containing mononuclear copper–peroxide adducts, there have been also examples of peroxide coordinated to multicopper sites. A structure of peroxide-bound tyrosinase determined to 1.8-Å resolution (PDB accession code 1WX2) [67] contains a peroxide ion in a bridging side-on coordination mode ($\mu\text{-}\eta^2\text{:}\eta^2$) with an O–O interatomic distance of 1.5 Å. Similarly, peroxide ligand bridges the dinuclear copper site of hemocyanin, although with a slightly shorter O–O bond of 1.4 Å (PDB accession code 1NOL, 2.4-Å resolution). Messerschmidt et al. [35] reported the 2.59-Å-resolution structure of ascorbate oxidase, in which peroxide binds within the trinuclear copper site. Peroxide was found terminally coordinated to the $\text{Cu}_2(\text{II})$ site (PDB accession code 1ASP), with a Cu(II)–O distance of 1.87 Å.

The enzyme CotA laccase from *Bacillus subtilis* represents another instance in which the structure of a multicopper–peroxide complex has been determined (PDB accession code 1W8E) [36]. In the peroxide-soaked CotA laccase, O_2^{2-} anion is coordinated within its trinuclear copper site (Cu_2 , Cu_3 , and Cu_4). Peroxide ligand bridges between $\text{Cu}_2(\text{II})$ and $\text{Cu}_3(\text{II})$. The $\text{Cu}_2(\text{II})\text{-O}_2$ and $\text{Cu}_3(\text{II})\text{-O}_1$ distances are 2.01 and 1.95 Å, respectively, and the peroxide also interacts with Cu_4 and one water molecule [the $\text{Cu}_4(\text{II})\text{-O}_1$ distance is 2.51 Å and the $\text{O}_2\text{-W}$ distance is 2.62 Å].

Summary and conclusions

Treatment of oxPHM with hydrogen peroxide results in the formation a complex in which peroxide anion coordinates side-on to the Cu_M active site. This Cu(II)-bound peroxy moiety interacts closely with a molecule of water, forming hydrogen bonds that stabilize the structure. DFT and QM–MM calculations indicate that this species is a copperbound doubly deprotonated peroxidate and that its energy is similar to that of its isomer, $\text{Cu}(\text{I})\text{-O}_2^-$.

On the basis of this and other evidence, we propose a modification of previously described mechanisms that provides a comprehensive rationale for previous observations and mechanistic proposals in this system. Besides satisfying the requirement of a substrate for the oxidation of both coppers by O₂ [27], the mechanism allows the hydroxylation of the substrate peptidylglycine using H₂O₂ as the source of both oxygen and reducing equivalents [52]. We are focusing our current efforts on the determination of the structure of the complex of oxPHM, hydrogen peroxide, and the slow-reacting substrate *N*-acetyldiiodotyrosyl-D-threonine peptide.

Supplementary Material

Refer to Web version on PubMed Central for supplementary material.

Acknowledgments

We acknowledge Jean Jakoncic and Vivian Stojanoff (beamline X6A of the National Synchrotron Light Source, Brookhaven National Laboratory) for assistance in the collection of X-ray diffraction data. We thank Sandra Gabelli and Mario Bianchet for assistance in the purification of the protein and crystallographic experiments. This work was supported by National Science Foundation grant MCB-920288 and National Institutes of Health grant DK-32949.

Abbreviations

AIM	Atoms in molecules
DFT	Density functional theory
MM	Molecular mechanical
oxPHM	Oxidized form of peptidylglycine α -hydroxylating monooxygenase
oxPHMcc	Oxidized catalytic core of peptidylglycine α -hydroxylating monooxygenase
PAM	Peptidylglycine α -amidating monooxygenase
PAL	Peptidyl- α -hydroxyglycine α -amidating lyase
PDB	Protein Data Bank
PHM	Peptidylglycine α -hydroxylating monooxygenase
PHMcc	Catalytic core of peptidylglycine α -hydroxylating monooxygenase
QM	Quantum mechanical

References

1. Merkler DJ, Kulathila R, Consalvo AP, Young SD, Ash DE. *Biochemistry*. 1992; 31:7282–7288. [PubMed: 1387319]
2. Noguchi M, Seino H, Kochi H, Okamoto H, Tanaka T, Hiramata M. *Biochem J*. 1992; 283(Pt 3):883–888. [PubMed: 1590776]
3. Prigge ST, Mains RE, Eipper BA, Amzel LM. *Cell Mol Life Sci*. 2000; 57:1236–1259. [PubMed: 11028916]
4. Eipper BA, Milgram SL, Husten EJ, Yun HY, Mains RE. *Protein Sci*. 1993; 2:489–497. [PubMed: 8518727]
5. Katopodis AG, May SW. *Biochemistry*. 1990; 29:4541–4548. [PubMed: 2372538]

6. Suzuki K, Ohta M, Okamoto M, Nishikawa Y. *Eur J Biochem.* 1993; 213:93–98. [PubMed: 8477737]
7. Glauder J, Ragg H, Rauch J, Engels JW. *Biochem Biophys Res Commun.* 1990; 169:551–558. [PubMed: 2357221]
8. Ouafik L, May V, Saffen DW, Eipper BA. *Mol Endocrinol.* 1990; 4:1497–1505. [PubMed: 1704483]
9. Eipper BA, Stoffers DA, Mains RE. *Annu Rev Neurosci.* 1992; 15:57–85. [PubMed: 1575450]
10. Czyzyk TA, Ning Y, Hsu MS, Peng B, Mains RE, Eipper BA, Pintar JE. *Dev Biol.* 2005; 287:301–313. [PubMed: 16225857]
11. Jiang N, Kolhekar AS, Jacobs PS, Mains RE, Eipper BA, Taghert PH. *Dev Biol.* 2000; 226:118–136. [PubMed: 10993678]
12. Prigge ST, Kolhekar AS, Eipper BA, Mains RE, Amzel LM. *Science.* 1997; 278:1300–1305. [PubMed: 9360928]
13. Prigge ST, Eipper BA, Mains RE, Amzel LM. *Science.* 2004; 304:864–867. [PubMed: 15131304]
14. Prigge ST, Kolhekar AS, Eipper BA, Mains RE, Amzel LM. *Nat Struct Biol.* 1999; 6:976–983. [PubMed: 10504734]
15. Siebert X, Eipper BA, Mains RE, Prigge ST, Blackburn NJ, Amzel LM. *Biophys J.* 2005; 89:3312–3319. [PubMed: 16100265]
16. Jaron S, Blackburn NJ. *Biochemistry.* 1999; 38:15086–15096. [PubMed: 10563791]
17. Rhames FC, Murthy NN, Karlin KD, Blackburn NJ. *J Biol Inorg Chem.* 2001; 6:567–577. [PubMed: 11472020]
18. Jaron S, Mains RE, Eipper BA, Blackburn NJ. *Biochemistry.* 2002; 41:13274–13282. [PubMed: 12403629]
19. Chen P, Bell J, Eipper BA, Solomon EI. *Biochemistry.* 2004; 43:5735–5747. [PubMed: 15134448]
20. Eipper BA, Quon AS, Mains RE, Boswell JS, Blackburn NJ. *Biochemistry.* 1995; 34:2857–2865. [PubMed: 7893699]
21. Freeman JC, Nayar PG, Begley TP, Villafranca JJ. *Biochemistry.* 1993; 32:4826–4830. [PubMed: 8387816]
22. Blackburn NJ, Rhames FC, Ralle M, Jaron S. *J Biol Inorg Chem.* 2000; 5:341–353. [PubMed: 10907745]
23. Francisco WA, Blackburn NJ, Klinman JP. *Biochemistry.* 2003; 42:1813–1819. [PubMed: 12590568]
24. Francisco WA, Knapp MJ, Blackburn NJ, Klinman JP. *J Am Chem Soc.* 2002; 124:8194–8195. [PubMed: 12105892]
25. Francisco WA, Merkler DJ, Blackburn NJ, Klinman JP. *Biochemistry.* 1998; 37:8244–8252. [PubMed: 9609721]
26. Tian G, Berry JA, Klinman JP. *Biochemistry.* 1994; 33:226–234. [PubMed: 8286345]
27. Freeman JC, Villafranca JJ. *J Am Chem Soc.* 1993; 115:4923–4924.
28. Crespo A, Marti MA, Roitberg AE, Amzel LM, Estrin DA. *J Am Chem Soc.* 2006; 128:12817–12828. [PubMed: 17002377]
29. Klinman JP. *J Biol Chem.* 2006; 281:3013–3016. [PubMed: 16301310]
30. Yoshizawa K, Kihara N, Kamachi T, Shiota Y. *Inorg Chem.* 2006; 45:3034–3041. [PubMed: 16562959]
31. Evans JP, Ahn K, Klinman JP. *J Biol Chem.* 2003; 278:49691–49698. [PubMed: 12966104]
32. Decker A, Solomon EI. *Curr Opin Chem Biol.* 2005; 9:152–163. [PubMed: 15811799]
33. Chen P, Solomon EI. *J Am Chem Soc.* 2004; 126:4991–5000. [PubMed: 15080705]
34. Kamachi T, Kihara N, Shiota Y, Yoshizawa K. *Inorg Chem.* 2005; 44:4226–4236. [PubMed: 15934751]
35. Messerschmidt A, Luecke H, Huber R. *J Mol Biol.* 1993; 230:997–1014. [PubMed: 8478945]
36. Bento I, Martins LO, Gato Lopes G, Armenia Carrondo M, Lindley PF. *Dalton Trans.* 2005:3507–3513. [PubMed: 16234932]

37. Shin DS, Didonato M, Barondeau DP, Hura GL, Hitomi C, Berglund JA, Getzoff ED, Cary SC, Tainer JA. *J Mol Biol.* 2009; 385:1534–1555. [PubMed: 19063897]
38. Kolhekar AS, Keutmann HT, Mains RE, Quon AS, Eipper BA. *Biochemistry.* 1997; 36:10901–10909. [PubMed: 9283080]
39. Otwinowski Z, Minor W. *Methods Enzymol.* 1997; 276:307–326.
40. Murshudov GN, Vagin AA, Dodson EJ. *Acta Crystallogr D Biol Crystallogr.* 1997; 53:240–255. [PubMed: 15299926]
41. Collaborative Computational Project N. *Acta Crystallogr D Biol Crystallogr.* 1994; 50:760–763. [PubMed: 15299374]
42. Frisch, MJ., et al. *Gaussian 03.* Wallingford: Gaussian; 2004.
43. Henkelman G, Arnaldsson A, Jonsson A. *Comput Mater Sci.* 2006; 36:354–360.
44. Crespo A, Scherlis DA, Marti MA, Ordejon P, Roitberg AE, Estrin DA. *J Phys Chem B.* 2003; 107:13728–13736.
45. Soler JM, Artacho E, Gale JD, Garcia A, Junquera J, Ordejon P, Sanchez-Portal D. *J Phys Condens Matter.* 2002:2745–2779.
46. Marti MA, Scherlis DA, Doctorovich FA, Ordejon P, Estrin DA. *J Biol Inorg Chem.* 2003; 8:595–600. [PubMed: 12644910]
47. Perdew JP, Burke K, Ernzerhof M. *Phys Rev Lett.* 1996; 77:3865–3868. [PubMed: 10062328]
48. Wang J, Cieplak P, Kollman P. *J Comput Chem.* 2000; 21:1049–1074.
49. Eichinger M, Tavan P, Hutter J, Parrinello M. *J Chem Phys.* 1999; 110:10452–10467.
50. Gubelmann MH, Williams AF. *Struct Bonding (Berl).* 1983; 55:1.
51. Chufan EE, Prigge ST, Siebert X, Eipper BA, Mains RE, Amzel LM. *J Am Chem Soc.* 2010; 132:15565–15572. [PubMed: 20958070]
52. Bauman AT, Yukl ET, Alkevich K, McCormack AL, Blackburn NJ. *J Biol Chem.* 2006; 281:4190–4198. [PubMed: 16330540]
53. Hrycay EG, Gustafsson JA, Ingelman-Sundberg M, Ernster L. *Eur J Biochem.* 1976; 61:43–52. [PubMed: 1735555]
54. Davydov R, Makris TM, Kofman V, Werst DE, Sligar SG, Hoffman BM. *J Am Chem Soc.* 2001; 123:1403–1415. [PubMed: 11456714]
55. Froland WA, Andersson KK, Lee SK, Liu Y, Lipscomb JD. *J Biol Chem.* 1992; 267:17588–17597. [PubMed: 1325441]
56. Wolfe MD, Lipscomb JD. *J Biol Chem.* 2003; 278:829–835. [PubMed: 12403773]
57. Gherman BF, Tolman WB, Cramer CJ. *J Comput Chem.* 2006; 27:1950–1961. [PubMed: 17019721]
58. Miller SM, Klinman JP. *Biochemistry.* 1985; 24:2114–2127. [PubMed: 3995006]
59. Osako T, Nagatomo S, Tachi Y, Kitagawa T, Itoh S. *Angew Chem Int Ed.* 2002; 41:4325–4328.
60. Mirica LM, Ottenwaelter X, Stack TD. *Chem Rev.* 2004; 104:1013–1045. [PubMed: 14871148]
61. Chen P, Fujisawa K, Solomon EI. *J Am Chem Soc.* 2000; 122:10177–10193.
62. Wada A, Harata M, Hasegawa K, Jitsukawa H, Masuda M, Mukai M, Kitagawa T, Einaga H. *Angew Chem Int Ed.* 1998; 37:798–799.
63. Maiti D, Lucas HR, Sarjeant AA, Karlin KD. *J Am Chem Soc.* 2007; 129:6998–6999. [PubMed: 17497785]
64. Maiti D, Sarjeant AA, Karlin KD. *J Am Chem Soc.* 2007; 129:6720–6721. [PubMed: 17474748]
65. Wilmot CM. *Biochem Soc Trans.* 2003; 31:493–496. [PubMed: 12773142]
66. Wilmot CM, Hajdu J, McPherson MJ, Knowles PF, Phillips SE. *Science.* 1999; 286:1724–1728. [PubMed: 10576737]
67. Matoba Y, Kumagai T, Yamamoto A, Yoshitsu H, Sugiyama M. *J Biol Chem.* 2006; 281:8981–8990. [PubMed: 16436386]

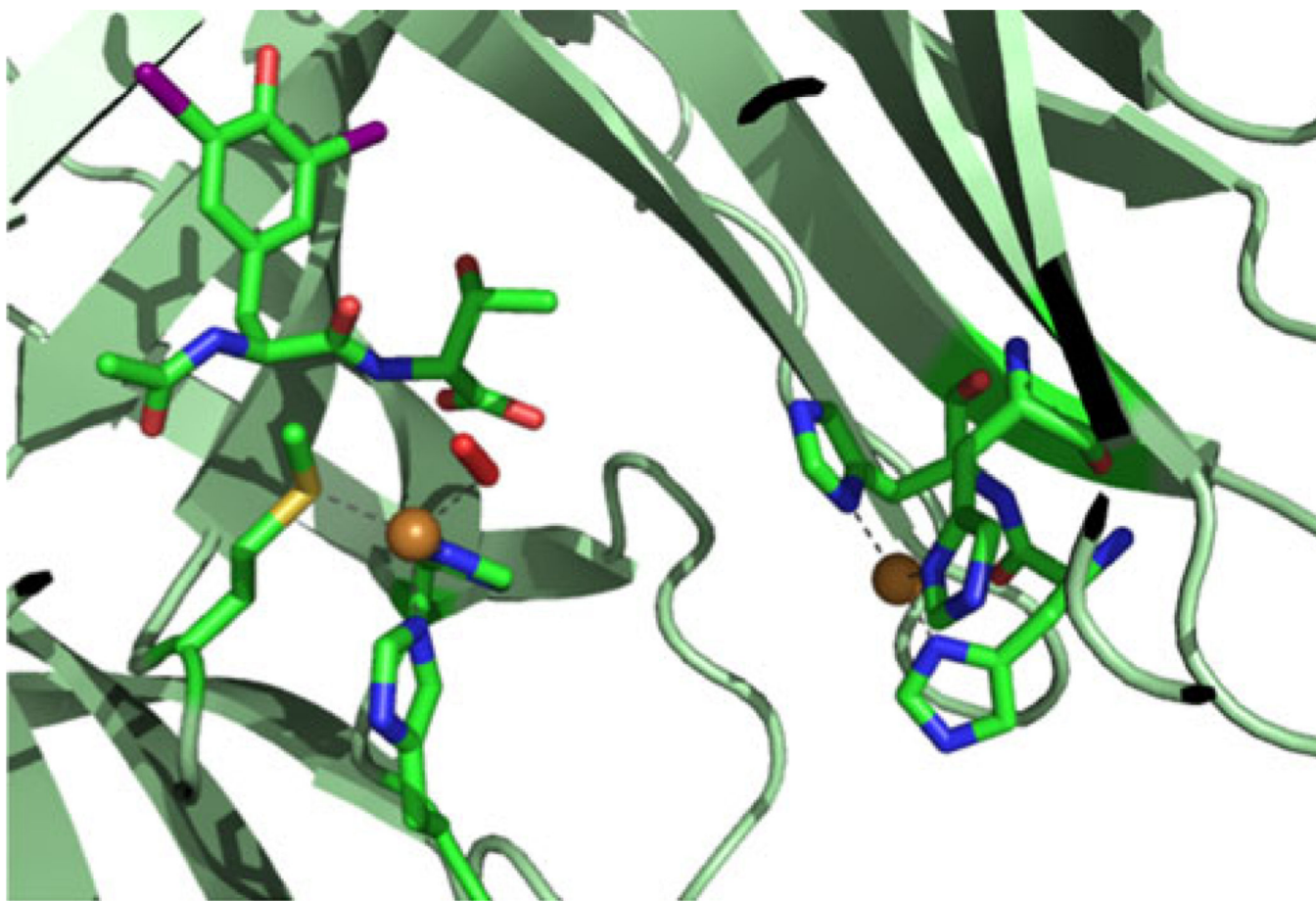


Fig. 1. X-ray structure of the ternary complex of reduced catalytic core of peptidylglycine α -hydroxylating monooxygenase (PHM) with dioxygen and the slow-reacting substrate *N*-acetyldiiodotyrosyl- D -threonine peptide [13]. Protein Data Bank (PDB) accession code 1SDW. The protein backbone is shown in *dark green*. The active site and the substrate carbon atoms are shown in *light green*, nitrogen atoms are shown *blue*, the sulfur atom is shown in *yellow*, copper atoms are shown in *gold*, and oxygen atoms are shown in *red*

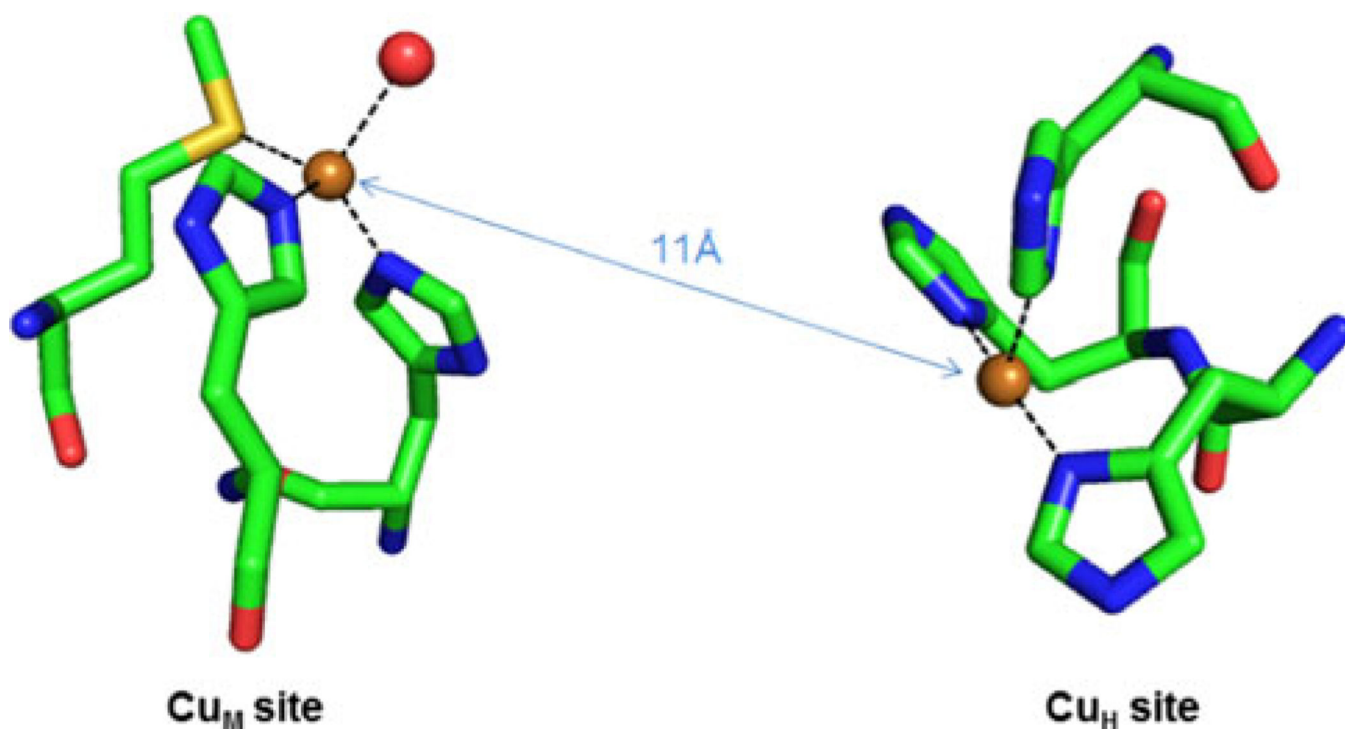


Fig. 2. Catalytic sites of PHM [12]. PDB accession code 1PHM. Carbon atoms are shown in *green*, nitrogen atoms are shown in *blue*, the sulfur atom is shown in *yellow*, copper atoms are shown in *gold*, and oxygen atoms are shown in *red*

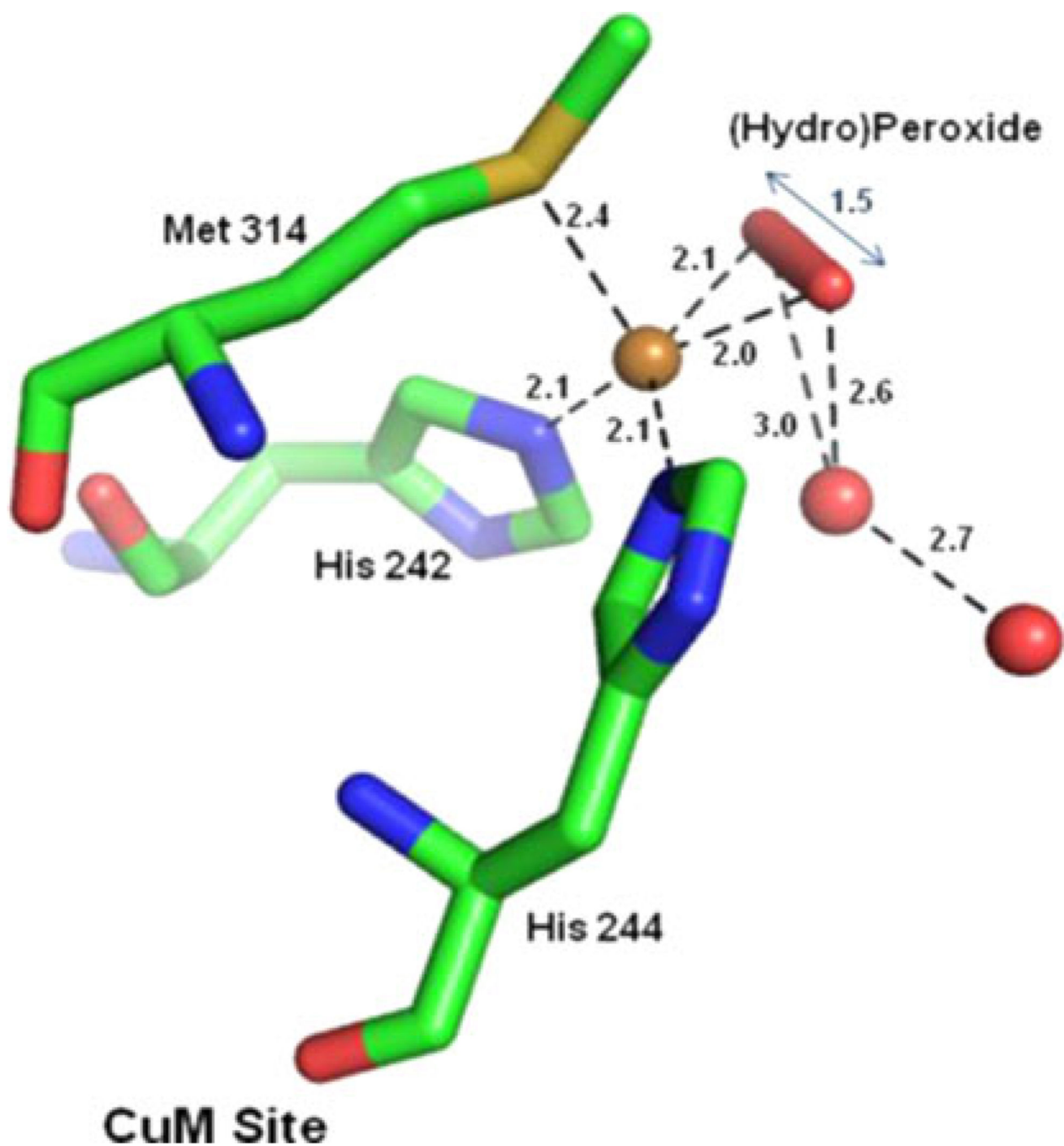


Fig. 3. Bond distances within the PHM Cu_M site coordinating the (hydro)peroxide ligand. PDB accession code 4E4Z. Carbon atoms are shown in *green*, nitrogen atoms are shown in *blue*, the sulfur atom is shown in *yellow*, copper atoms are shown in *gold*, and oxygen atoms are shown in *red* (the peroxide ligand is represented by a stick model, whereas the oxygen atoms of water are shown as spheres)

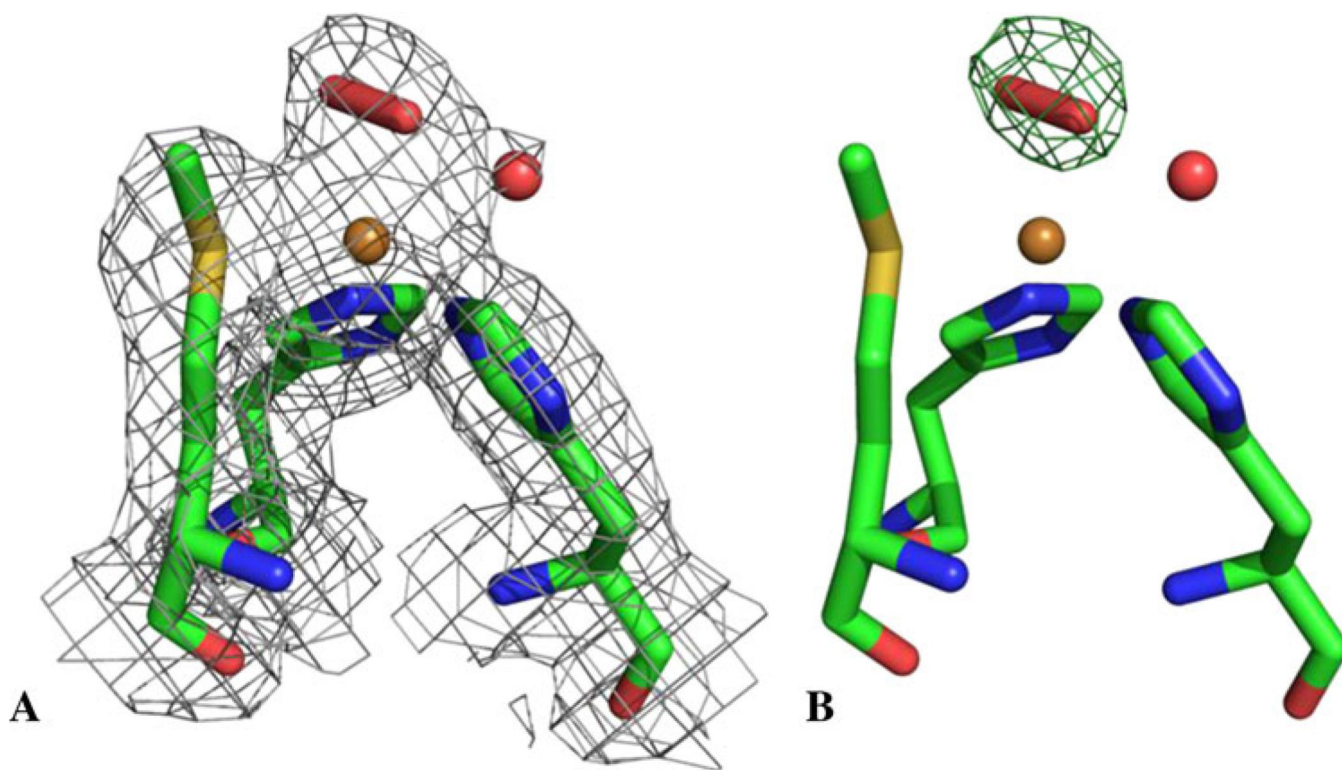


Fig. 4.

a Cu_M site of the H₂O₂-bound catalytic core of PHM. The $2mF_{obs} - DF_{calc}$ map is contoured at 1.0σ and is represented by a *gray mesh*. **b** The omit map ($mF_o - DF_c$) was calculated with Refmac 5.0; the *green mesh* represents a contour at 6σ . PDB accession code 4E4Z. Carbon atoms are shown in *green*, nitrogen atoms are shown in *blue*, sulfur atoms are shown in *yellow*, copper atoms are shown in *gold*, and oxygen atoms are shown in *red*

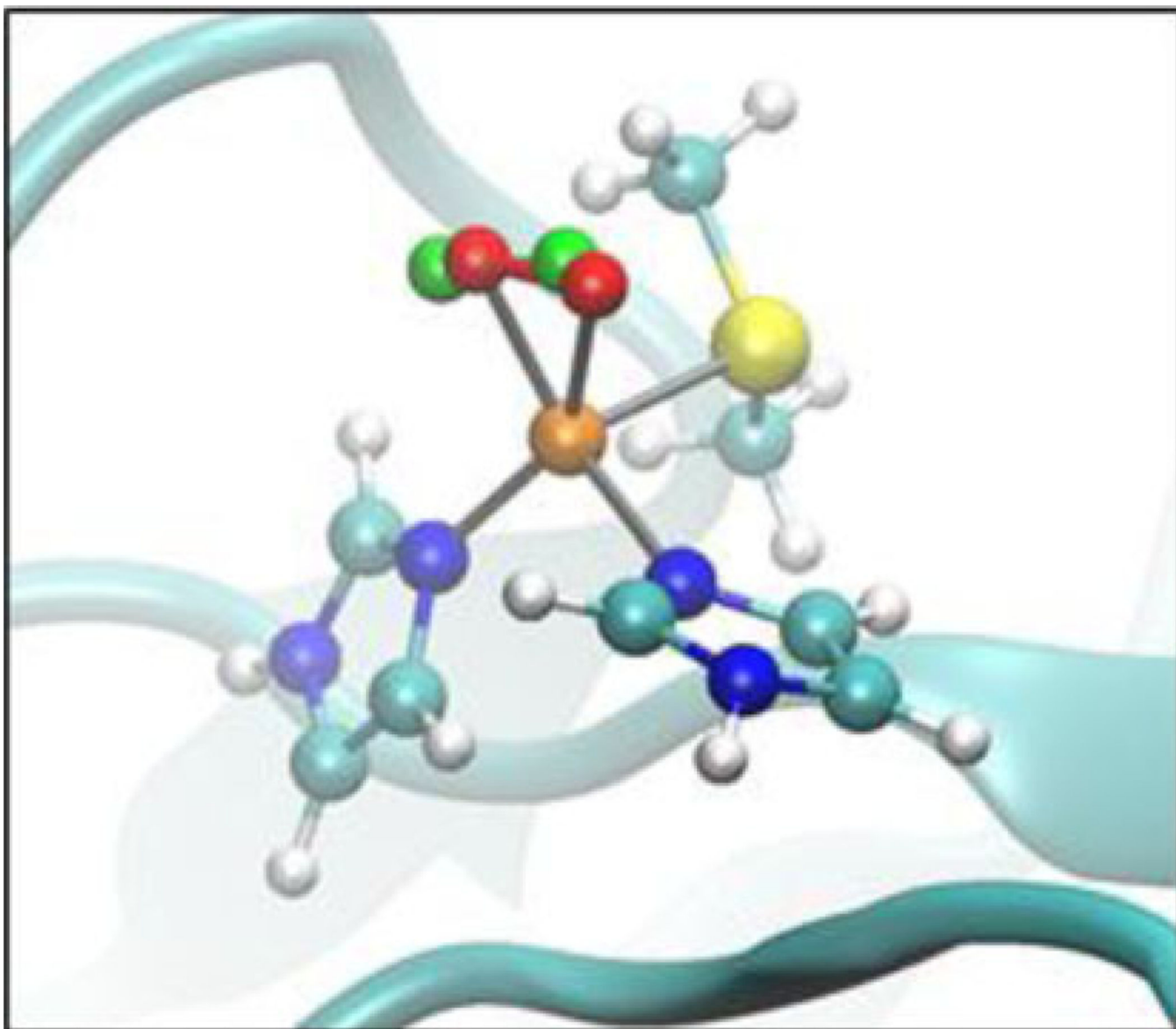
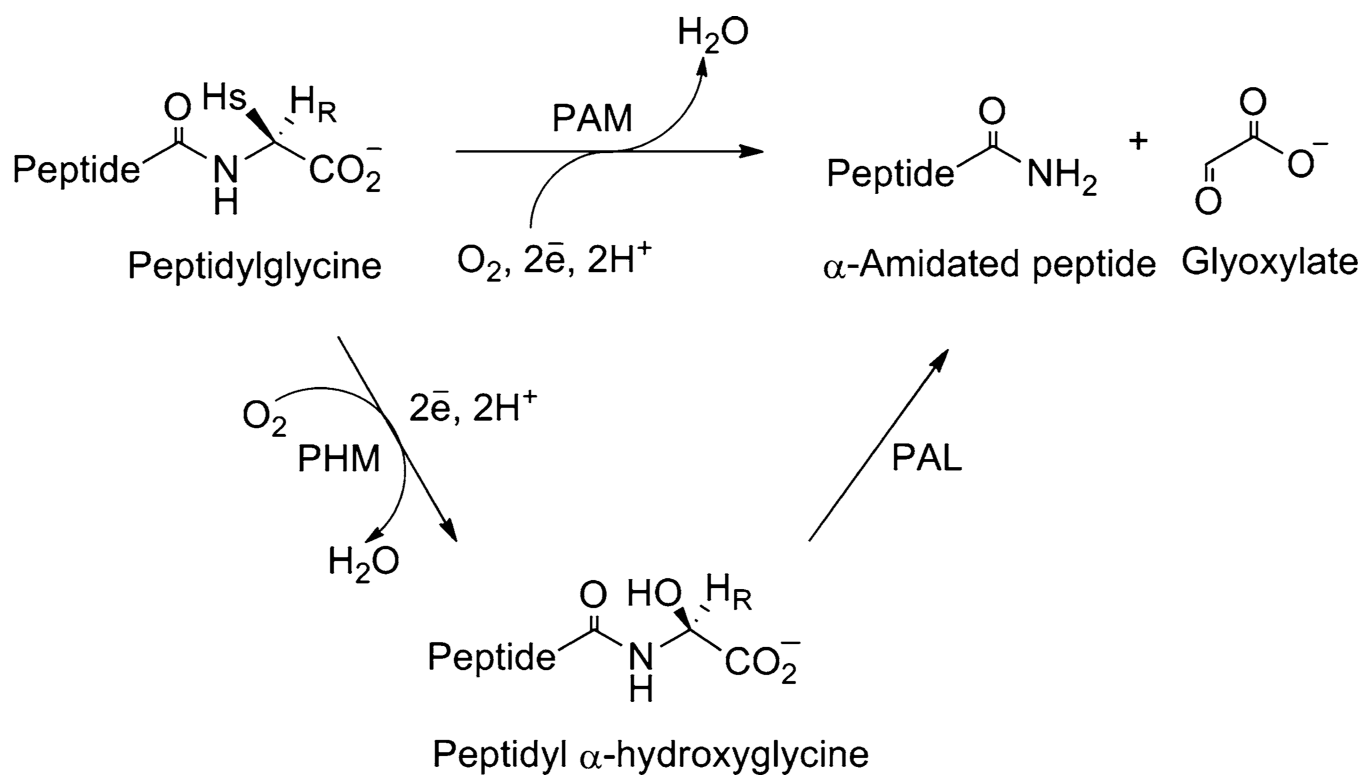
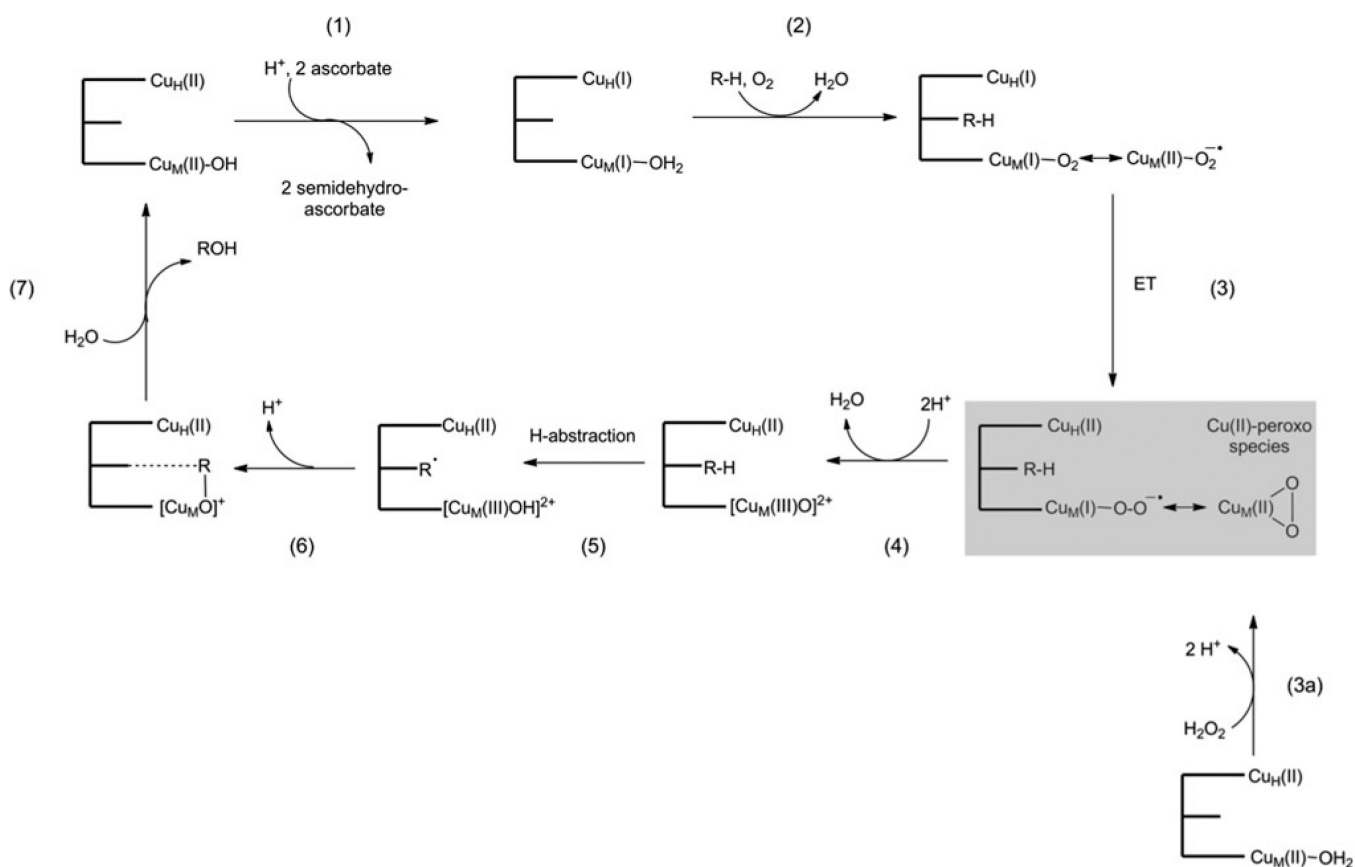


Fig. 5. Optimized structures of the CuM site obtained by quantum mechanical–molecular mechanical calculation. The peroxo-bound optimized structure is shown in *red* and the position of the H₂O₂-derived ligand in the crystal structure is shown in *green*



Scheme 1.
Catalytic reaction of peptidylglycine α -amidating monooxygenase (*PAM*)

**Scheme 2.**

Mechanism of the peptidylglycine α -hydroxylating monooxygenase (PHM) reaction including formation of reactive $\text{O}_2/\text{H}_2\text{O}_2$ -derived species of the Cu_M of PHM

Table 1

Crystallographic data collection and refinement statistics for the oxidized form of the catalytic core of peptidylglycine α -hydroxylating monooxygenase (oxPHMcc) complexed with H₂O₂ (Protein Data Bank, PDB, accession code 4E4Z)

Unit cell parameters (Å)	a = 68.5 b = 68.5 c = 81.5
Space group	<i>P</i> 2 ₁ 2 ₁ 2 ₁
Molecules/asymmetric unit	1
Wavelength (Å)	1.00
Resolution (Å)	1.98
Observed reflections	315,278
Unique reflections	26,738
Redundancy	11.8 (9.4)
Completeness (%)	97.4 (95.1)
$\langle I \rangle / \sigma \langle I \rangle$	53.6 (3.3)
<i>R</i> _{sym} (%)	6.3 (69.2)
Refinement	
<i>R</i> / <i>R</i> _{free} (%)	21/24
Stereochemistry	
Rms bond length (Å)	0.010
Rms angles (°)	1.2
Model composition	
Amino acids	312
Cu/Ni	2/1
Peroxide	1
Glycerol	4
Water	150
Total atoms	2,612

Table 2

Experimental and theoretical relevant geometrical parameters of the CuM site in peptidylglycine α -hydroxylating monooxygenase

Distance (Å)	Experimental	Optimized structure, model system			Optimized structure
		L_3Cu_M (II)-H ₂ O ₂	L_3Cu_M (II)-HO ₂ ⁻	L_3Cu_M (II)-O ₂ ²⁻	QM-MM optimization
	α PHHMc-H ₂ O ₂ (PDB ID 4E4Z)				L_3Cu_M (II)-O ₂ ²⁻
Cu-O ₁	2.00	2.08	1.85	1.94	2.04
Cu-O ₂	2.13	2.68	2.82	1.95	2.14
O ₁ -O ₂	1.49	1.47	1.43	1.44	1.39
Cu-O ₁ -O ₂	70	96	118	68	74
Cu-O ₂ -O ₁	69			69	67

MM molecular mechanical, QM quantum mechanical